

Thermal and Acceleration Load Analysis of New 122 mm Rocket Propellant Grain

Nikola Gligorijević¹⁾
Saša Antonović¹⁾
Saša Živković¹⁾
Bojan Pavković¹⁾
Vesna Rodić¹⁾

In order to achieve very strong inter-ballistic requirements, a unusual free standing rocket motor propellant grain was designed, with variable channel diameter. Due to its very high length, it was expected for the grain to be exposed to dangerous combination of different loads during the design phase. Structural analysis of viscoelastic propellant grain is always very complex and it differs substantially from an elastic analysis, because the propellant mechanical properties depend on temperature and strain rate. The most complex case in the analysis occurs when multiple loads operate simultaneously. In this paper, the structural analysis has been done during the initial period of rocket flight, when the grain is under very fast load due to acceleration and at the same time under a slow load due to surface pressure, created as a result of temperature dilatation. In the absence of data on mechanical properties of the new propellant composition, the properties over the whole time-temperature range were estimated comparing by a similar composition that have been completely tested earlier. Using finite element method (ANSYS program) two different design solutions were examined and the more reliable one was adopted.

Key words: rocket, 122 mm calibre, rocket engine, propellant grain, thermal load, acceleration, viscoelasticity, structural analysis, tensile strength, damage, reliability, finite elements method.

Nomenclature

a_T	– Time-temperature shift factor
D	– Cumulative damage
E	– Modulus, initial, tangent, elasticity
R	– Strain rate,
t	– Time
$\varepsilon, \varepsilon_0$	– Strain, Initial strain,
$\varepsilon_m, \varepsilon_{m0}$	– Ultimate (Allowable) strain, Initial strain
ξ	– Reduced time
$\eta(t)$	– Propellant aging factor
$\eta_E, \eta_\sigma, \eta_\varepsilon$	– Aging factor for modulus, stress, strain
σ_m	– Tensile strength (Ultimate stress)
$\sigma_{m0}, \sigma_m(t)$	– Initial strength, Time-dependent strength

Introduction

BASED on a designing task to develop a rocket motor for a 122 mm artillery rocket with maximum range of 50 km, a

very long free standing propellant grain was defined (≈ 2200 mm) with circular central channel (Fig.1).

The basic requirements of internal ballistics demand from the rocket motor designer to find design solutions in order to achieve necessary theoretical thrust distribution, but also to prevent practical occurrence of erosive burning.

For this kind of propellant grain, radial combustion is the only possible type. Furthermore, due to the internal-ballistic request to provide the sufficient value of total impulse, it was also necessary to provide a sufficiently long burning time of the rocket motor. In this way the possibility to make a star shaped channel was eliminated, as well as the burning on the outer side of the grain. Then, the first internal-ballistic problem arised because the burning surface distribution in the hollow tube channel is highly progressive [1,2], although approximately neutral burning was required. The second internal-ballistic problem was erosive burning [3-6], which almost always occurs in very long propellant grains. Finally, a unusual propellant grain design is proposed (Fig.1), with variable channel diameter that should solve both problems of internal ballistics.



Figure 1. Sectional view of 122 mm rocket motor

¹⁾ Military Technical Institute (VTI), Ratka Resanovića 1, 11132 Belgrade, SERBIA
Correspondence to: Nikola Gligorijević; e-mail: nikola.gligorijevic@gmail.com

This very long propellant grain design has opened a problem of its structural resistance upon the effects of different types of loads and very high risk of grain failure [7-9]. The structural analysis showed that successful realization of structural reliability is probably much more complex than the achievement of internal ballistics requirements.

Structural analysis of a viscoelastic body, like propellant grain, is quite complex, and its end result, which is reflected through the safety factor (margin of safety) or probability of grain failure is usually less reliable than the result of an elastic analysis. Free standing propellant grain is exposed to various loads, such as due to extended polymerization, due to temperature dilatation and surface pressure on the grain joints with supporting elements in the rocket motor chamber, due to transportation and handling, and finally due to working pressure and rocket acceleration. Mechanical properties of viscoelastic rocket propellant strongly depend on temperature and strain rate [7-11]. There are various methods for analysis that use some mathematical transformation, that allow to a structural analyst to resolve the problem in a similar way as for the elastic body [12-14]. However, such structural analysis procedure applies only if it is possible to express the stress and strain fields due to some external load in closed mathematical form [7, 9, 15, 16]. However, usually only a quasi-elastic analysis is made, which differs from the elastic analysis only because it includes the temperature and strain rate dependence of the mechanical properties of the propellant as well as the stress field in the propellant grain [8,9].

More complex is structural analysis when the propellant grain is at the same time under two or more loads that act by different rates. This leads to different strain rates in the grain. Since the mechanical properties of viscoelastic bodies depend on the strain rate, they will differ in the case of each individual load. For example, tensile strength in the case of acceleration load is different than tensile strength of the propellant in the case of temperature load.

This can be easily understood if the loads act at various time intervals. But if the loads are acting at the same time, it is not possible to define the equivalent value of the ultimate propellant mechanical properties and it is necessary to make a satisfactory model for the analysis. This model has not been explicitly discussed in literature, although there are recommendations for its solution [7,9], similar to the model for the analysis of cumulative damage [17,18], which relies on a model for damage in fatigue [19].

In the case of considered propellant grain, after a period of ignition, when the pressure is stabilized in the whole free volume of the motor chamber, the mechanical impact of pressure on the propellant charge is reduced. Then the second critical stage begins and the slow temperature load acts alongside with very fast acceleration load. The rocket motor designer has estimated that at this stage a critical load appears at the point where support elements touch and pressure the surface of the grain.

This phase is discussed in this paper. Based on the results of structural analysis, among the two proposed design solutions of the propellant grain, the one with higher reliability has been adopted.

Safety factor estimate in the case of multiple loads

In the structural analysis of an elastic body, the values of ultimate mechanical properties (tensile strength and ultimate strain) are nearly constant. Their dependence on temperature and strain rate over the operating range is usually negligible.

Then, the safety factor can be simply represented as the ratio between ultimate strength (σ_m) and the resulting stress (σ_0) due to the action of a number of different loads:

$$\nu = \frac{\sigma_m}{\sigma_0} \quad (1)$$

In the case of a viscoelastic body, the mechanical properties depend on temperature and strain rate. When different types of external loads act simultaneously upon the body, they produce different stresses, $\sigma_1(t)$, $\sigma_2(t)$, $\sigma_3(t)$... Different types of loads also produce different strain rates in the viscoelastic body, so the tensile strengths differ. In this case it is not possible to define the equivalent tensile strength, so it is not possible to apply the model for safety factor determination like in the case of an elastic body.

Theoretically, for the linear-viscoelastic material, the mathematical model for the calculation of cumulative damage and service life can be applied. [9, 17-20].

According to the Miner's law of cumulative damage [19] applied on rocket propellants [9], total damage caused by different loads can be displayed by following expression:

$$D = \sum d_i = \sum \frac{t_i}{t_{fi}} \quad (2)$$

d_i - current damage added by the i -th individual load

t_i - time exposure to i -th stress level

t_{fi} - mean time to failure at i -th stress level

Following the same logic, the total damage under the action of multiple loads can be displayed by expression: [20, 21]:

$$D = \sum \frac{\sigma_i}{\sigma_{mi}} \quad (3)$$

σ_i - stress level caused by the i -th load

σ_{mi} - tensile strength corresponding to the i -th load

In this way, the action of each load is considered individually. Total current damage (D) actually shows how much of the total capacity of resistance to failure is used up in the moment of multiple loads action. Theoretically, if this value is less than 1, there will be no failure of the body. The safety factor is equal to the reciprocal of the total current damage:

$$\nu = \frac{1}{D} \quad (4)$$

This principle is applied in the analysis in this paper.

The task of propellant grain structural analysis

Based on the internal-ballistic analysis, a very long propellant grain was made (Fig.1) with high length to diameter ratio ($l > 2200$ mm, $L/D \approx 20$). Due to rather high coefficient of thermal expansion of the composite rocket propellant, the grain length dilatation is very large ($\Delta l \approx 15$ mm) over the whole temperature range of the rocket motor use (-40, +50°C).

A better view onto the proposed propellant grain design can be seen in Fig.2 where it is shown in a shortened form with two cross-sections lengthwise.

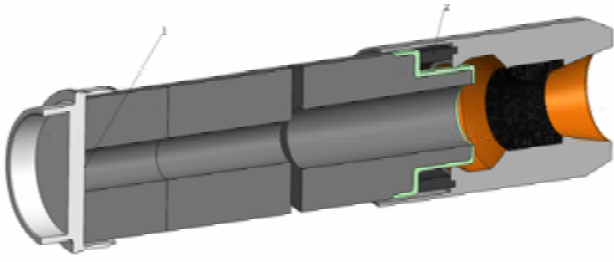


Figure 2. Propellant grain position in the rocket motor

A potential problem can occur because it is necessary for the grain to be in stable position in the motor chamber in all conditions before use. The grain should be securely fixed over the whole service life, during handling, transportation and storage. It is necessary to prevent any possibility of the grain displacement, regardless the change in its length due to outside temperature and to avoid high stresses of the grain that could lead to its failure.

Rocket motor designer has suggested that the right front side of the grain should rely onto the compensator of temperature dilatation (Pos. 2) on the back side of the motor, near the nozzle. This compensator is designed to have a sufficient flexibility to accept major changes in the grain length.

In Fig.2 there is a design solution where the left front side of the propellant grain is relied onto the flange (Pos.1). From the point of production, this solution is probably better, but the grain is under higher stresses upon the external loads. Preliminary analysis has shown that it would be possible to change the way of reliance on the left front side of the grain to get an important stress reduction, but that other solution is more complex for production.

If the propellant grain withstands the first pressure peak during the ignition phase, at the beginning of the steady state of motor combustion the impact of pressure onto the stress state in the free standing grain will become negligible [7-9].

Then there are two important loads acting onto the grain in the initial phase of the rocket flight.

At first, there is a very slow load due to the temperature dilatation [7-9, 18] that creates high surface pressure in the front sides of the grain. When the rocket motor is at the lower limit temperature in the range (-40°C), the length of the grain is minimum, and the surface pressure on its front side is small. When the temperature reaches the upper limit ($+50^{\circ}\text{C}$), the surface pressure on the front of the grain increases to its maximum.

The second important load is the additional surface pressure due to very fast acceleration load.

These two completely different loads act simultaneously, so it is necessary to apply the presented model of current damage summation. The task of structural analysis was to determine whether the total surface pressure is too large, resulting in possible damage of the propellant. Two possible design solutions were considered and the better one has been chosen.

Experiment

During the internal-ballistic analysis, in the design phase, rocket motor designer usually considers different propellant compositions, as well as possible grain designs in order to achieve proper ballistic properties of the motor.

At this stage, the designer usually does not have any information about the mechanical properties of the propellant, or has only the most basic data obtained by measuring on the tensile tester at standard conditions ($+20^{\circ}\text{C}$, 50 mm/min)

[13, 17]. In the considered case, at his/her own request, the designer has received additional basic data from standard speed tensile tests (50 mm/min) at extreme temperatures (-40°C , $+50^{\circ}\text{C}$).

Uniaxial constant rate tests were done by tensile tester Instron-1122 and the results are presented in Fig.3.

Standard tensile tests are not sufficient for detailed structural analysis of the grain. In the process of production they are usually used for a quick assessment of the propellant and for comparison with other propellants.

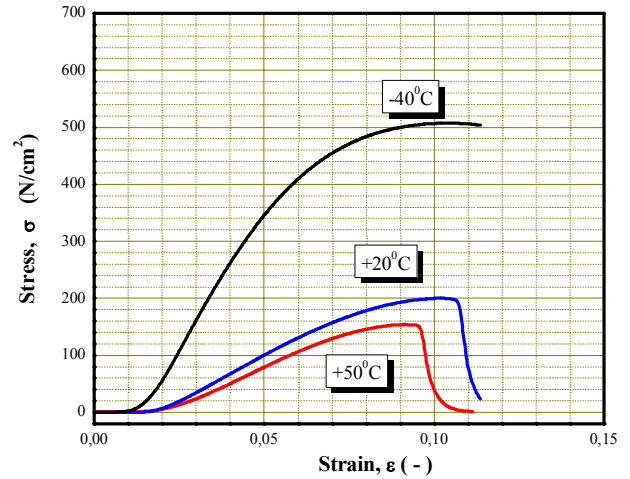


Figure 3. Standard rate tensile tests

Tabela 1. Mechanical properties of the propellant in standard rate conditions (50 mm/min)

T	ϵ_m	σ_m	E_0
$^{\circ}\text{C}$	%	daN/cm ²	daN/cm ²
-40	10,41	50,71	1066,18
+20	10,16	19,98	335,33
+50	9,14	15,38	281,68

Complete mechanical characterization includes a long-term process of tensile tests at a number of different temperature and strain rate test modes [8, 10, 13] in order to determine mechanical properties of the propellant in a wide range of operating conditions.

It is possible to approximately define dependence of the new propellant mechanical properties in all conditions, comparing the results of standard tests with complete results of a similar composite propellant from the MTI database.

The procedure and results of the complete mechanical characterization of the HTPB-based composite propellants from database were shown in the paper [11]. These measurements were carried out all over the temperature range between -60°C and $+50^{\circ}\text{C}$ and tensile tester crosshead speeds between 0.2 and 1000 mm/min.

From the papers [11, 22] the following dependencies of the propellant from database were taken:

1. Tensile strength master curve:

$$\log \sigma_m \cdot \frac{T_0}{T} = 1,110 - 0,1289 \cdot \log\left(\frac{t}{a_T}\right) \quad (5)$$

2. Ultimate strain master curve

$$\epsilon_m (\%) = 6,663 + 10,514 \cdot e^{-2 \cdot \left(\frac{\xi + 1,366}{7,119}\right)^2}; \quad \xi = \frac{t}{a_T} \quad (6)$$

3. Time-temperature shift factor

$$\log a_T = -\frac{4,0 \cdot (T - 293)}{127 + T - 293} \quad (7)$$

4. Initial modulus master curve

$$\log E \cdot \frac{T_0}{T} = 2,20 - 0,138 \cdot \log\left(\frac{t}{a_T}\right) \quad (8)$$

Each of these diagrams has been made on the basis of uniaxial tensile tests at more than 100 different test modes. Standard tests (50 mm/min) were done at three different temperatures: (-40, +20, +50°C), which are equal to three different regimes. When the results are entered into the existing master diagrams of the propellant from database, it is possible to make approximate functional dependencies for the new propellant.

For this propellant there is no data on temperature dependence of temperature shift factor $a_T(T)$, but for the similar composite propellant it was assumed that the factor $a_T(T)$ has the same distribution like the propellant from database. This assumption is acceptable because the values of $a_T(T)$ are very similar for comparable polymer compositions [23].

The axes of master diagrams are defined in literature [7-11]. On the ordinates there are logarithmic values of normalized tensile strength $\log(\sigma_m \cdot T_0/T)$, modulus $\log(E \cdot T_0/T)$, and percentage values of ultimate strain ε_m .

Reduced time is defined as:

$$\xi = \frac{t}{a_T} = \frac{1}{R \cdot a_T} \quad (9)$$

- R (-) - strain rate
- a_T - time-temperature shift factor

In the standard test, JANNAF specimen is used [8, 11], tensile tester speed $v = 50$ mm/min. Strain rate is:

$$R = \frac{v(\text{mm/min})}{60 \cdot l_0(\text{mm})} = \frac{50}{60 \cdot 68,6} = 0,012148 \quad (10)$$

$l_0 = 68.6$ mm - basic length of the propellant specimen

$$\log \xi = -\log R - \log a_T \quad (11)$$

At all the three abscissas there are the values of reduced time ξ . Reference temperature is conventionally 20°C.

The three measured points are plotted into characteristic diagrams of the mechanical properties, along with the master curves from database. These values are shown in Table 2.

Table 2. Mechanical properties of the new propellant

T	$\log \xi$	ε_m	$\log(\sigma_m \cdot \frac{T_0}{T})$	$\log(E_0 \cdot \frac{T_0}{T})$
°C		%	daN/cm ²	daN/cm ²
-40	-1,666	10,41	1,805	3,127
+20	1,9155	10,16	1,301	2,525
+50	2,680	9,14	1,145	2,407

Tensile strength is shown in Fig.4.

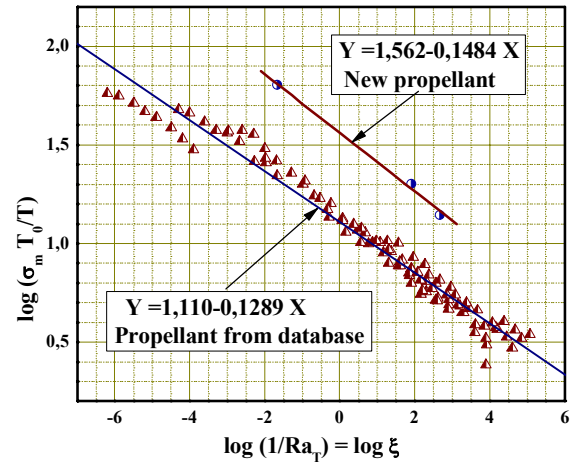


Figure 4. Tensile strength

The initial modulus is shown in Figure 5:

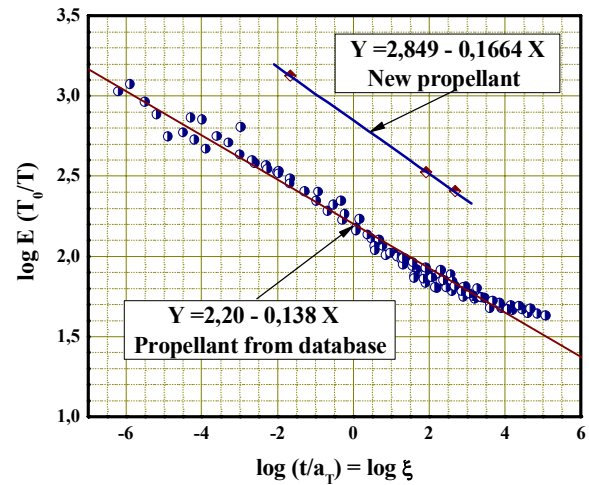


Figure 5. Initial modulus

It is seen in Figures 4 and 5 that the tensile strength and initial modulus master curves are approximately linear. It can be assumed that similar dependencies for master curves of the new propellant are also linear.

Analogy between the two propellants is less visible in the case of ultimate strain (Fig.6) because dispersion of the points is very large. On the basis of the three measurement points it is not possible to determine the layout of the approximate master curve of the new propellant.

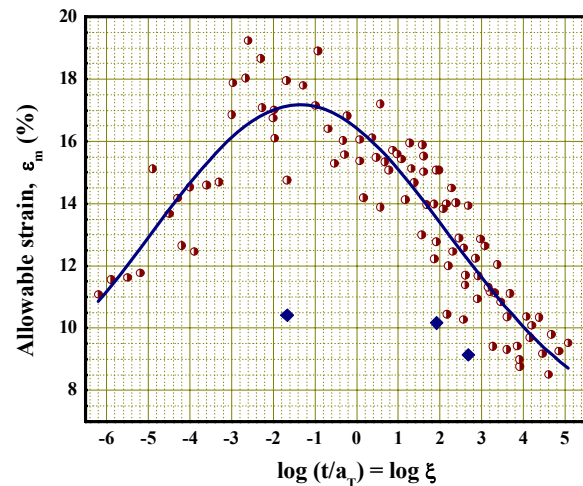


Figure 6. Ultimate strain

Based on the approximate expressions in Figures 4 and 5 for the tensile strength and initial modulus of the new propellant, it is possible to calculate and analyze the real stresses and strains in the propellant grain under various types of loads, especially temperature and acceleration loads in order to make the safety factor assessment.

Analysis

Tensile strengths under the effects of two different loads

This brief preliminary analysis is carried out on the same principle as for the elastic body [8, 9, 16]. Applying some of the known methods of the elastic analysis, such as the finite element method, structural analyst defines potential critical zones in the grain, with the greatest stresses and strains. The essential difference is that the mechanical properties are variable and depend on the load conditions.

The first step in the analysis was to determine the strain rates under the effects of two different loads, temperature and acceleration.

Schematic representation of a propellant grain deformation due to the axial acceleration is shown in Fig. 7.

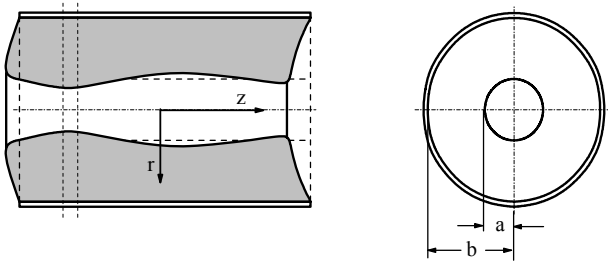


Figure 6. Grain deformations under axial acceleration

Expressions for the calculation of longitudinal deformation of a propellant grain with a circular channel, due to the axial acceleration were previously successfully used in literature [7, 9, 14]:

$$\Delta l = \frac{3\rho \cdot g \cdot N}{2 \cdot E} \cdot \left[\frac{b^2 - r^2}{2} - a^2 \cdot \ln \frac{b}{r} \right] \quad (12)$$

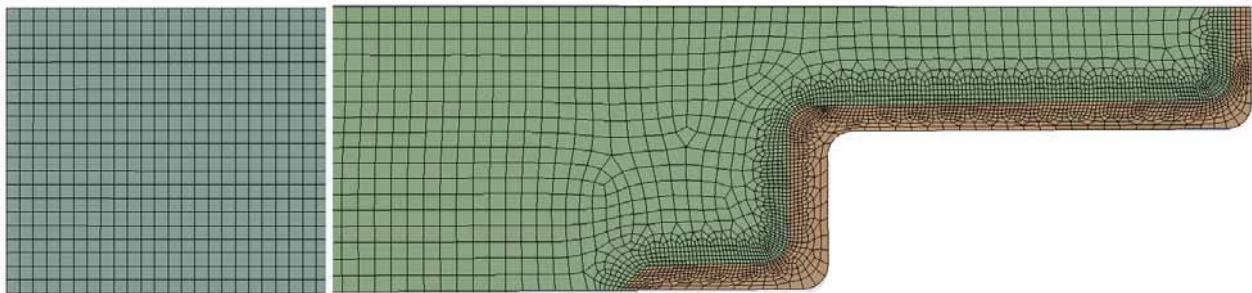


Figure 8. Finite element grid

When the numerical values are inserted into the expression (12), excluding the unknown value of the modulus E , it gets the following form:

$$\Delta l(\text{cm}) = \frac{0,82}{E(\text{daN/cm}^2)} \quad (13)$$

Δl	- axial displacement
a	- radius of the hollow tube, $a = 17,00 \text{ mm}$
b	- outer radius of the grain, $b = 59,25 \text{ mm}$
r	- arbitrary radius of the grain
$g \cdot N$	- axial acceleration
ρ	- propellant density, $\rho = 1,762 \text{ g/cm}^3$
E	- propellant modulus

On the basis of projected properties of the missile, the value of axial acceleration is approximately $g \cdot N = 38,5 \text{ g}$.

In the expression (8) the unknown values are radius r and modulus E . The radius value was adopted on the basis of preliminary qualitative analysis, which has shown that the most loaded zone of the grain is at the right end of the propellant grain (Fig. 8) at the contact with the compensator of temperature dilatation.

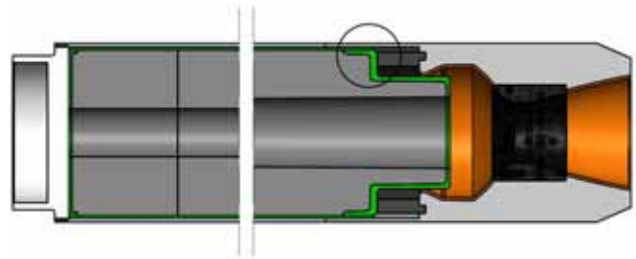


Figure 7. The most stressed zone of the propellant grain

This zone is approximately about half the grain thickness, at the radius $r \approx 0,5 \cdot (a + b) \approx 38 \text{ mm}$. The value of modulus is unknown, it depends on the strain rate, which is also unknown at this stage of analysis.

Splitting the propellant grain into the finite elements is shown in Fig. 9, with special attention to the grain connections to the other elements of the rocket motor on the right side of the grain. The results were obtained using ANSYS software [24].

Two-dimensional analysis was performed. To generate the network, function generator "Curvature Size" was used, which adapts the network to the curvature of the object. The model was defined with the elements in form of rectangles, minimum of 1mm edge, thus achieving optimum in terms of speed and accuracy of analysis. In zones of the propellant grain where the increased stress concentration was expected, the network was further fragmented.

Based on the value of displacement Δl (13) and the basic length of propellant grain $l \approx 220 \text{ cm}$, the value of strain can be determined, but again only depending on the modulus.

$$\varepsilon(-) = \frac{\Delta l}{l_0} = \frac{\Delta l}{200(\text{cm})} = \frac{0,82}{220 \cdot E(\text{daN/cm}^2)}$$

$$\varepsilon(-) = \frac{0,0037}{E(\text{daN/cm}^2)} \quad (14)$$

The rocket reaches its maximum acceleration approximately in ($t_a \approx 35 \text{ ms}$). It is assumed that the maximum displacement of the grain due to acceleration is reached approximately at the same time. Dividing the maximum strain with the acceleration time (t_a) the reference value of the strain rate is obtained:

$$\frac{d\varepsilon}{dt} \approx \frac{\varepsilon}{t_a} = \frac{0,0037}{E \cdot t_a} = \frac{0,0037}{E \cdot 35 \cdot 10^{-3}} \quad (15)$$

$$\frac{d\varepsilon}{dt} (s^{-1}) = \frac{0.106}{E(\text{daN/cm}^2)}$$

The strain rate dependence on modulus (11) is undefined because the propellant modulus is unknown. Otherwise, the value of the modulus as a material property is defined by the approximate expression in Fig. 5:

$$\log(E \cdot \frac{T_0}{T}) = 2,849 - 0,1664 \cdot \log(\frac{1}{\dot{\varepsilon} \cdot a_T}) \quad (16)$$

Solving the system of equations (15) and (16) we can determine the values of modulus and strain rate. Modulus values depend on temperature, so they have to be determined for three different temperatures, the standard ($+20^\circ\text{C}$) and the two extreme limits in the temperature region of the rocket motor use (-40 and $+50^\circ\text{C}$).

In the case of another load, caused by a very slow temperature dilatation, maximum theoretical elongation and strain of the propellant grain can be achieved in the range between the two temperature extremes (-40 to $+50^\circ\text{C}$), but this range is not relevant for this calculation, as these are two seasonal temperatures with a wide time interval between.

During a day over the season, temperature difference is not greater than about 20°C , so the longitudinal deformation of the propellant grain is:

$$\varepsilon = \frac{\Delta l}{l_0} = \alpha \cdot \Delta T$$

$$\varepsilon = 0,93 \cdot 10^{-40} C^{-1} \cdot 20^\circ C \approx 0,186 \cdot 10^{-6} \quad (17)$$

α - coefficient of thermal expansion for the composite propellant [13, 17]

Under real operating conditions, this temperature change ($\Delta T \approx 20^\circ\text{C}$) can happen in 8 hours. Then, the strain rate is:

$$\dot{\varepsilon} = \frac{\varepsilon}{\Delta t} = \frac{0,186 \cdot 10^{-6}}{8h}$$

$$\dot{\varepsilon} = \frac{0,186 \cdot 10^{-6}}{8 \cdot 60 \cdot 60} = 0,646 \cdot 10^{-11} s^{-1} \quad (18)$$

The strain rate determination under temperature load is not fully reliable. It is usually based on an estimate of the structural analyst. This strain rate is so small that the approximate expressions in the diagrams 4 and 5 give very low values for modulus and tensile strength. Therefore, when such a case occurs and the value of reduced time is unrealistically high, the structural analyst should adopt

maximum measured value for the reduced time in the master curve diagrams (Figures 4, 5) [13, 17], and the appropriate values of the modulus and tensile strength.

In this case, for the maximum temperature ($+50^\circ\text{C}$) the value $\log \xi \approx 6,0$ has been adopted. The values of reduced time for other characteristic temperatures ($+20, -40^\circ\text{C}$) are determined based on difference due to time-temperature shift factor a_T .

The values of modulus and tensile strength under the acceleration and temperature loads are shown in Tables 3 and 4, at the three characteristic temperatures ($-40, +20, +50^\circ\text{C}$).

Based on the values of strain rates and reduced times for the two different loads, the values of modulus were determined by expression (16) while the tensile strength was determined using the approximate expression in Fig. 4:

$$\log(\sigma_m \cdot \frac{T_0}{T}) = 1,562 - 0,1484 \cdot \log(\frac{1}{\dot{\varepsilon} \cdot a_T}) \quad (19)$$

It is seen in Tables 3 and 4 that the tensile strengths at -40°C are about 3 times greater than the tensile strengths at $+50^\circ\text{C}$, in both cases.

In addition, the values of tensile strengths under the two loads differ in almost 100%. In the case of pressure load, this difference may be even greater.

Table 3. Mechanical properties under acceleration load

T	E	$\log \xi$	σ_m	$\sigma_m(p)$
$^\circ\text{C}$	daN/cm ²	s	daN/cm ²	
-40	543,5	0,085	28,18	56.36
+20	204,0	3,241	12,05	24.10
+50	172,5	3,933	10,49	20.98

Table 4. Mechanical properties under thermal load

T	E	$\log \xi$	σ_m	$\sigma_m(p)$
$^\circ\text{C}$	daN/cm ²	s	daN/cm ²	
-40	361,0	1,154	19,55	39,10
+20	115,1	4,736	7,23	14,46
+50	94,7	$\sim 5,5$	6,14	12,28

In the last columns on the right of both Tables 3 and 4, there are the values of ultimate strength in the case of pressure load, which is usually accepted to be twice the value of the tensile strength [8, 25].

Load, damage and safety factor analysis

Using the finite element method, two different design solutions were considered for supporting the propellant grain in the rocket motor chamber. The values of the surface pressure were considered at the propellant grain joints with supporting elements.

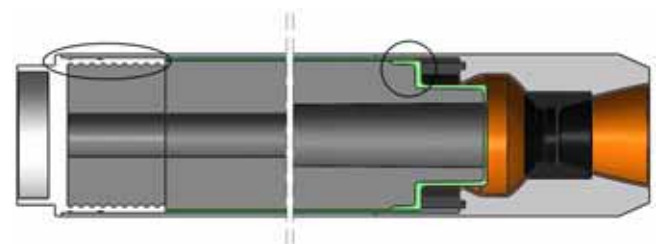


Figure 9. Modified design of the grain connection

The first design solution (option 1) is shown in Fig.8 and the critical zone of the grain is marked.

In Fig.10, the modified design solution of the grain reliance is shown (option 2). The left side of the grain is connected by a threaded joint to the supporting elements. In the second design option, the critical zone with the largest surface pressure is on the right side of the grain, too.

Version No.1

Fig.11 shows the stress distribution along the entire propellant grain. The maximum stress occurs on the right front side of the grain.

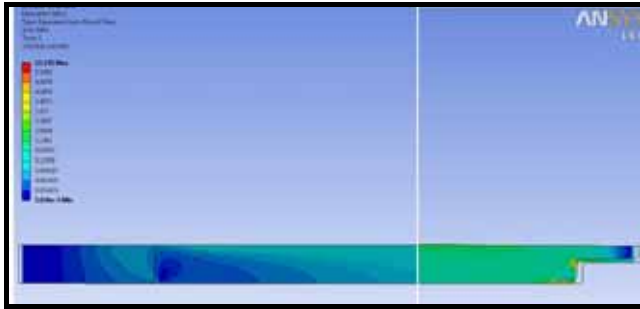


Figure 10. Stress distribution along the grain (version 1)

Table 5 shows the values of the stresses caused by temperature $\sigma(T)$ and acceleration $\sigma(a)$ in the critical zone for the option No. 1 (Fig.8). Comparing the actual stresses with the ultimate pressure stresses, the values of partial current damages due to individual loads are obtained. The total damages at the two extreme temperatures are shown in the last column on the right.

Table 5. Damages caused by different loads - Version 1

T	$\sigma(a)$	$\sigma(T)$	$d(a)$	$d(T)$	$\sum d$
$^{\circ}C$	daN/cm ²		-	-	-
-40	15,37	0,43	0,273	0,013	0,286
+50	11,4	4,2	0,543	0,342	0,885

The value of the total damage at + 50°C is considered too high (0,885) and is close to 1. This means that this design solution is near the resistance limit and is not sufficiently reliable.

Version No.2

Fig.12 shows the stress distribution along the modified version of the propellant grain. The maximum stress also occurs on the right front side of the grain, but the stress distribution along the grain is more uniform.

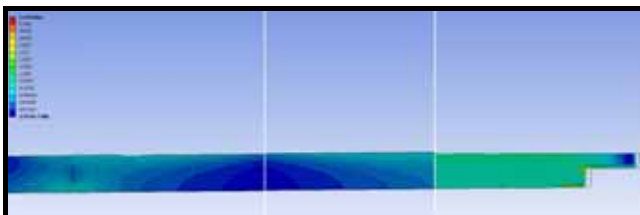


Figure 12. Stress distribution along the grain (version 2)

The stresses and current damages caused by temperature $\sigma(T)$ and acceleration $\sigma(a)$ in the critical zone for the option No. 2 are shown in the Tab. 6.

Table 6. Damages caused by different loads - Version 2

T	$\sigma(a)$	$\sigma(T)$	$d(a)$	$d(T)$	$\sum d$
$^{\circ}C$	daN/cm ²		-	-	-
-40	8,17	0,43	0,273	0,013	0,286
+50	7,50	4,2	0,357	0,342	0,699

Analysis of safety factor (ν) is made using the model of single "current damages" (d) caused by individual loads. Then, individual values of two different current damages were simply summarized to get the total current damage:

$$d = d(a) + d(T)$$

$$d = \frac{\sigma(a)}{\sigma_m(a)} + \frac{\sigma(T)}{\sigma_m(T)} \quad (20)$$

Safety factor for this design solution is:

$$\nu = \frac{1}{d} \approx \frac{1}{0,699} = 1,43. \quad (21)$$

The result obtained in this preliminary analysis indicates that one of the two considered design solutions of the propellant grain support is possible (version 2). In Fig. 12 dark fields along the grain can be seen, which indicate the zones with lower stresses. But it is not enough because the numerical value of the total damage is still high, and the safety factor is not big enough as we would like, due to lack of reliability of this type of analysis.

This means that more detailed analysis is needed. Additional consideration of possible structural changes of the grain in the zones of attachment to the supporting elements of the motor is necessary, as well as a modification of the propellant composition in order to increase the ultimate mechanical properties.

Conclusion

An example of the preliminary structural analysis of a rocket propellant grain in the design phase is presented. Special characteristics of the analysis are presented, based on the viscoelastic nature of the rocket propellant.

An example of a short preliminary structural analysis is presented, when two completely different loads act simultaneously onto the viscoelastic propellant grain, resulting in the problem of defining a failure criterion, since the allowable mechanical properties of viscoelastic materials strongly depend on the strain rate. These cases were not considered in literature.

In the absence of sufficient mechanical properties data of the rocket propellant, a simplified method was applied and compared to a propellant from database. It is shown that whenever this approximate method can be applied, by comparing with a similar propellant composition, this could enable a structural analyst to avoid a lengthy and complex process of complete mechanical characterization.

References

- [1] SUTTON, G.P., BIBLARZ, O.: *Rocket Propulsion Elements*, Eighth edition. John Wiley & Sons inc. ISBN: 978-0-470-08024-5, 2010.
- [2] NASA: Solid propellant grain design and internal ballistics, NASA Space Vehicle Design Criteria SP-8076, 1972.
- [3] WIMPRESS, R.N.: *Internal Ballistics of Solid-Fuel Rockets*, McGraw-Hill Book Company, New York-Toronto-London, 1950.

- [4] KING, K. MERRILL.: *Erosive burning of composite solid propellants*, Atlantic Research Corporation. Air Force Office of Scientific Research, AFOSR-TR-81-0395, AD A098088, 1981.
- [5] ФАХРУТДИНОВ, И.Х., КОТЕЛЬНИКОВ, А.В.: *Конструкция и проектирование ракетных двигателей твердого топлива*, Москва, "Машиностроение", 1987.
- [6] MUKUNDA, H.S., PAUL, P.J.: *Universal Behaviour in Erosive Burning of Solid Propellants*, Combustion and Flame: 1997, 109, pp. 224-236.
- [7] WILLIAMS, M.L., BLATZ, P.J., SCHAPERY, R.A.: *Fundamental Studies Relating to Systems Analysis of Solid Propellants*, Final report GALCIT 101, Guggenheim Aero. Lab., Pasadena, California, 1961.
- [8] FITZGERALD, J.E., HUFFERD, W.L.: *Handbook for the Engineering Structural Analysis of Solid Propellants*, CPIA publication 214, 1971.
- [9] *Solid propellant grain structural integrity analysis*, NASA Space Vehicle Design Criteria SP-8073, 1973.
- [10] LANDEL, R.F., SMITH, T.L.: *Viscoelastic Properties of Rubberlike Composite Propellants and Filled Elastomers*, ARS Journal, 1960, Vol.31, No.5, pp.599-608.
- [11] GLIGORIJEVIĆ, N., RODIĆ, V., ŽIVKOVIĆ, S., PAVKOVIĆ, B., NIKOLIĆ, M., KOZOMARA, S., SUBOTIĆ, S.: *Mechanical Characterization of Composite Solid Rocket Propellant based on hydroxy-terminated polybutadiene*, Chemical Industry, 2015. DOI:10.2298/HEMIND150217067G.
- [12] WILLIAMS, M.L.: *Structural Analysis of Viscoelastic Materials*, AIAA Journal, California Institute of Technology, Pasadena, May 1964, pp. 785-798.
- [13] GLIGORIJEVIĆ, N.: *Strukturalna analiza pogonskih punjenja raketnih motora sa čvrstim gorivom*, Vojnotehnički Institut, Beograd, NTI, 2013, Vol.XLIX, No.1, ISSN 1820-3418, ISBN 978-86-81123-59-1.
- [14] МОСКВИТИН, В.В.: *Сопротивление вязко-упругих материалов*, Наука, Москва 1972.
- [15] GLIGORIJEVIĆ, N., RODIĆ, V., JEREMIĆ, R., ŽIVKOVIĆ, S., SUBOTIĆ, S.: *Structural Analysis Procedure for a Case Bonded Solid Rocket Propellant Grain*, Scientific Technical Review, ISSN 1820-0206, 2011, Vol.61, No.1, pp.1-11.
- [16] GLIGORIJEVIĆ, N.: *Prilog strukturalnoj analizi vezanog pogonskog punjenja raketnog motora sa čvrstom pogonskom materijom*, Magistarski rad, University of Belgrade, Faculty of Mechanical Engineering, Belgrade, SERBIA, 1989.
- [17] GLIGORIJEVIĆ, N.: *Istraživanje pouzdanosti i veka upotrebe raketnih motora sa čvrstom pogonskom materijom (Solid propellant rocket motor reliability and service life research)*, Ph.D. Dissertation, Military Academy, Belgrade, SERBIA, 2010.
- [18] HELLER, R.A., SINGH, M.P.: *Thermal Storage Life of Solid-Propellant Motors*, Journal of Spacecraft and Rockets, 1983, Vol.20, No.2, pp.144-149.
- [19] MINER, M.A.: *Cumulative Damage in Fatigue*, Journal of Applied Mechanics, 1945, Vol.12, pp.159-164.
- [20] GLIGORIJEVIĆ, N., ŽIVKOVIĆ, S., RODIĆ, V., SUBOTIĆ, S., GLIGORIJEVIĆ, I.: *Effect of Cumulative Damage on Rocket Motor Service Life*, Journal of Energetic Materials, 2015, Vol.33, No.4, DOI:10.1080/07370652.2014.970245
- [21] GLIGORIJEVIĆ, N., ŽIVKOVIĆ, S., KOVAČEVIĆ, N., DIMITRIJEVIĆ, N., PAVKOVIĆ, B., PAVIĆ, M., RODIĆ, V.: *Analysis of Viscoelastic Behavior of a Filled Elastomer Under Action of Different Loads*, Chemical Industry, 2016. DOI:10.2298/HEMIND160627042G.
- [22] ANTONOVIĆ, S., GLIGORIJEVIĆ, N., MILOJKOVIĆ, A., SUBOTIĆ, S., ŽIVKOVIĆ, S., PAVKOVIĆ, B.: *An example of propellant grain structural analysis under the thermal and acceleration loads*, 7th International Scientific Conference on Defensive Technologies OTEH 2016, 06-07. October 2016, Belgrade, SERBIA, ISBN 978-86-81123-82-9, pp.300-306.
- [23] WILLIAMS, M.L., LANDEL, R.F., FERRY, J.D.: *The Temperature Dependence of Relaxation Mechanisms in Amorphous Polymers and Other Glass-forming Liquids*, J. Am. Chem. Soc., 1955, 77 (14), pp 3701-3707, DOI: 10.1021/ja01619a008.
- [24] ANSYS®, Documentation for Release 14.0, Help System, ANSYS, Inc.
- [25] THRASHER, D.I., HILDRETH, J.H.: *Structural Service Life Estimate for a Reduced Smoke Rocket Motor*, Journal of Spacecraft, 1982, Vol.19, No.6, pp.564-570.

Received: 06.06.2016.

Accepted: 12.09.2016.

Analiza opterećenja pogonskog punjenja rakete 122 mm usled temperature i ubrzanja

U cilju ispunjenja strogih unutar-balističkih zahteva projektovano je slobodno pogonsko punjenje raketnog motora posebnog oblika, sa promenljivim prečnikom kanala. U fazi projektovanja je procenjeno da će pogonsko punjenje, zbog svoje velike dužine, biti izloženo snažnim kombinacijama različitih opterećenja. Strukturna analiza viskoelastičnog pogonskog punjenja je uvek vrlo složena i suštinski se razlikuje od elastične analize, pošto mehaničke osobine pogonske materije zavise od temperature i brzine deformacije. Najsloženiji slučaj u analizi se javlja kada višestruka opterećenja deluju istovremeno. U ovom radu je izvršena strukturalna analiza punjenja u početnoj fazi leta rakete, kada je pogonsko punjenje pod uticajem veoma brzog opterećenja usled ubrzanja i istovremeno površinskog pritiska nastalog kao posledica veoma sporog opterećenja usled temperaturnih dilatacija. U nedostatku podataka o mehaničkim osobinama novog goriva, osobine u celom vremensko-temperaturnom rasponu su određene poređenjem sa jednim sličnim sastavom koji je ranije kompletno ispitan. Primenom metode konačnih elemenata (program ANSYS) razmatrane su dve različite varijante konstrukcije pogonskog punjenja i usvojeno je pouzdanije rešenje.

Ključne reči: raketa, kalibar 122 mm, raketni motor, pogonsko punjenje, termičko opterećenje, ubrzanje, viskoelastičnost, strukturalna analiza, zatezna čvrstoća, oštećenje, pouzdanost, metoda konačnih elemenata.

Анализ нагрузок пропеллента зерна пороховых ракет 122-мм на тепловую и ускоряющую нагрузку

Для достижения очень высоких и строгих межбаллистических требований было разработано необычное ракетное топливо для свободного ракетного двигателя специальной формы, с переменным диаметром канала. На этапе проектирования предполагалось, что ракетное топливо, из-за своей большой длины, будет подвергаться воздействию мощного сочетания различных нагрузок. Структурный анализ вязкоупругого ракетного топлива всегда очень сложный и существенно отличается от упругого анализа, поскольку механические свойства ракетного топлива

зависят от температуры и скорости деформации. Наиболее сложный случай в анализе возникает, когда несколько нагрузок действуют одновременно. В данной работе выполнен структурный анализ ракетного топлива в начальном этапе полёта ракеты, когда метательный заряд находится под воздействием высокоскоростных нагрузок из-за ускорения и одновременного поверхностного давления, созданного в результате очень медленной нагрузки из-за расширения температуры. При отсутствии данных о механических качествах нового топлива, свойства в течение всего временного температурного диапазона оценивались по сравнению с аналогичным составом, который ранее был полностью проверен и испытыван. С помощью метода конечных элементов (программный комплекс ANSYS) рассматриваны два различных варианта конструктивных решений ракетного топлива и принято более надёжное решение.

Ключевые слова: ракета, калибр 122 мм, ракетный двигатель, ракетное топливо, тепловая нагрузка, ускорение, вязкоупругость, структурный анализ, прочность на разрыв, повреждение, надёжность, метод конечных элементов

Analyse de la charge chez la charge propulsive de la fusée de 122mm par rapport à la température et à l'accélération

Dans le but d'accomplir les exigences sévères de balistique intérieure on a conçu une charge propulsive libre pour le moteur à fusée de forme particulière à diamètre variable du canal. Au cours de la conception on a estimé que la charge propulsive due à sa grande longueur serait exposée aux fortes combinaisons de diverses charges. L'analyse structurale de la charge propulsive viscoélastique est toujours très complexe et se différencie essentiellement de l'analyse élastique parce que les propriétés mécaniques de la matière propulsive dépendent de la température et de la vitesse de déformation. Le cas le plus complexe dans l'analyse se produit quand les charges multiples agissent simultanément. Dans ce papier on a fait l'analyse structurale de la charge dans la phase initiale du vol de fusée lorsque la charge propulsive est sous une charge très rapide causée par l'accélération et la pression superficielle simultanée due à la charge très lente de la dilatation de température. Dans l'absence des données sur les propriétés mécaniques du propergol nouveau les propriétés sont déterminées dans toute la portée de temps et de température et comparées avec une composition similaire examinée entièrement avant. En utilisant la méthode des éléments finis (programme ANSYS) on a considéré deux différentes solutions pour la construction de la charge propulsive et on a adopté la solution plus sûre.

Mots clés: fusée, calibre 122mm, moteur à fusée, charge propulsive, charge thermique, accélération, viscoélasticité, analyse structurale, résistance à la tension, endommagement, fiabilité, méthode des éléments finis.